ELSEVIER

Journal of Loss Prevention in the Process Industries 13 (2000) 327–340

Journal of Loss Prevention in the process industries

www.elsevier.com/locate/jlp

Flammability of methane, propane, and hydrogen gases

Kenneth L. Cashdollar [a,*], Isaac A. Zlochower [a], Gregory M. Green [a], Richard A. Thomas [a], Martin Hertzberg [1,b]

[a] *Pittsburgh Research Laboratory, National Institute for Occupational Safety and Health, Pittsburgh, PA, USA*
[b] *Copper Mountain, Colorado, USA*

Abstract

This paper reports the results of flammability studies for methane, propane, hydrogen, and deuterium gases in air conducted by the Pittsburgh Research Laboratory. Knowledge of the explosion hazards of these gases is important to the coal mining industry and to other industries that produce or use flammable gases. The experimental research was conducted in 20 L and 120 L closed explosion chambers under both quiescent and turbulent conditions, using both electric spark and pyrotechnic ignition sources. The data reported here generally confirm the data of previous investigators, but they are more comprehensive than those reported previously. The results illustrate the complications associated with buoyancy, turbulence, selective diffusion, and ignitor strength versus chamber size. Although the lower flammable limits (*LFLs*) are well defined for methane (CH_4) and propane (C_3H_8), the *LFLs* for hydrogen (H_2) and its heavier isotope deuterium (D_2) are much more dependent on the limit criterion chosen. A similar behavior is observed for the upper flammable limit of propane. The data presented include lower and upper flammable limits, maximum pressures, and maximum rates of pressure rise. The rates of pressure rise, even when normalized by the cube root of the chamber volume ($V^{1/3}$), are shown to be sensitive to chamber size. Published by Elsevier Science Ltd.

Keywords: Gas; Flammable; Explosion; Flammability

1. Introduction

Previous gas flammability limit data were obtained mainly in 5 to 10 cm diameter flammability tubes, with lengths ten to thirty times the diameter, using spark ignition sources. Those flammability data are summarized in three Bureau of Mines bulletins (Coward & Jones, 1952; Zabetakis, 1965; Kuchta, 1985). In those previous tests, a gas mixture in a vertical tube was ignited and flame propagation was determined by a visual criterion. To measure upward flame propagation, the gas mixture would be ignited at the bottom of the tube and the flame would travel upward to the top of the tube. To measure downward flame propagation, the gas mixture would be ignited at the top of the tube and the flame would travel downward.

The purpose of the present research was to obtain fundamental gas flammability data by measuring the pressure rise in closed chambers of different volumes. The gases studied were methane (CH_4), propane (C_3H_8), normal hydrogen (H_2), and its heavier isotope, deuterium (D_2). The flammability data are essential for a quantitative risk assessment of the explosion hazard associated with the use of these gases. These gases are widely used (except D_2) and have widely varying molecular weights and diffusivities relative to oxygen. The effect of relative diffusivity of fuel and oxygen on the behavior of mixtures near the flammability limits can influence those limits and the appropriate criteria for distinguishing between a flammable and nonflammable concentration (Hertzberg 1982, 1989). Methane, propane, and hydrogen are also used as standards with which other flammable gases can be compared. The gas flammability tests reported here were conducted from the mid-1980's through the 1990's at the Pittsburgh Research Laboratory[2] (PRL) in 20 L and 120 L chambers using standard

* Corresponding author. Tel.: +1-412-386-6753; fax: +1-412-386-6595.
E-mail address: kgc0@cdc.gov (K.L. Cashdollar).
[1] Private consultant, retired from the U.S. Bureau of Mines

[2] Many of these data were collected while the PRL was part of the U.S. Bureau of Mines, before its transfer to the National Institute for Occupational Safety and Health (NIOSH) in October 1996.

0950-4230/00/$ - see front matter. Published by Elsevier Science Ltd.
PII: S0950-4230(99)00037-6

test procedures developed by the PRL for similar studies. Some earlier data from an 8 L cylindrical chamber and a 25.5 m^3 sphere at PRL are also included. The flammability data reported include lower (lean) flammable limits, upper (rich) flammable limits, peak explosion pressures, and maximum rates of pressure rise. The tests were performed at ambient temperature and pressure under both quiescent and turbulent conditions. Some of the data in this report were presented previously in Hertzberg, Cashdollar and Zlochower (1988) and in two contract reports to the Department of Energy and its site contractors (Cashdollar, Hertzberg, Zlochower, Lucci, Green, & Thomas (1992) and Zlochower, Cashdollar, & Green (1997)).

2. Test chambers and experimental procedures

The flammability data for this report were obtained in 8 L, 20 L, 120 L, and 25 500 L (25.5 m^3) chambers. The majority of the data are from the 120 L spherical chamber shown in Fig. 1. The internal diameter of the chamber is 60 cm, and its pressure rating is 69 bar. Instrumentation included a sensitive strain gauge pressure transducer to measure the partial pressures as the gases were added and mixed, two strain gauge pressure transducers to monitor the explosion pressure, and a silicon photodiode flame sensor. The strain gauges had a response time of ~1 ms. For some of the tests, a piezoelectric pressure transducer (with a response time of ~1 μs) was used. The pressure transducers were usually mounted on the top and bottom flanges of the chamber as shown in Fig. 1, but sometimes they were mounted on the sides of the chamber during the various series of tests over several years. For most of the tests, the flame sensor was mounted on the top flange to observe the flame radiation and, more importantly, to detect the spark radiation. This would confirm that the spark ignition source was working properly for tests in which the mixture did not ignite. For some of the tests, a fine wire thermocouple near the top of the chamber was used to record the gas flame temperature. The spark electrodes were located slightly below center. An internal fan was used to mix the gases.

Two "20 L" chambers (Fig. 2) were also used for the gas flammability tests. One had a volume of 19.4 L and the other had a volume of 20.8 L. For this report, both will be referred to as 20 L chambers. Each is a nearly spherical vessel made of 13 mm thick stainless steel (type 304) with a pressure rating of 21 bar. The approximate dimensions are 35 to 37 cm in height and 30 cm in diameter. Two strain gauges were used to measure the explosion pressure. For some of the tests, a thermocouple was used to measure the gas temperature. The sapphire windows allowed visual observation of the tests. There were also ports with ball valves for connection to a vacuum pump, vent, and a more sensitive pressure transducer for gas addition by partial pressure. There were ports with needle valves for connection to sources of compressed dry air and the fuel gases. There was a solenoid controlled port on the bottom for the rapid introduction of compressed air to assist in mixing the

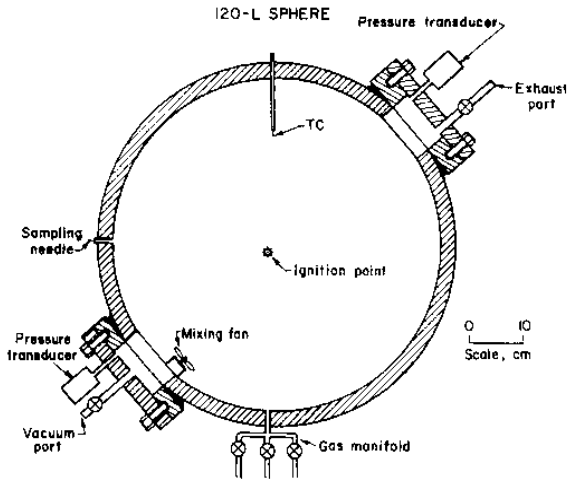

Fig. 1. 120 L flammability test sphere.

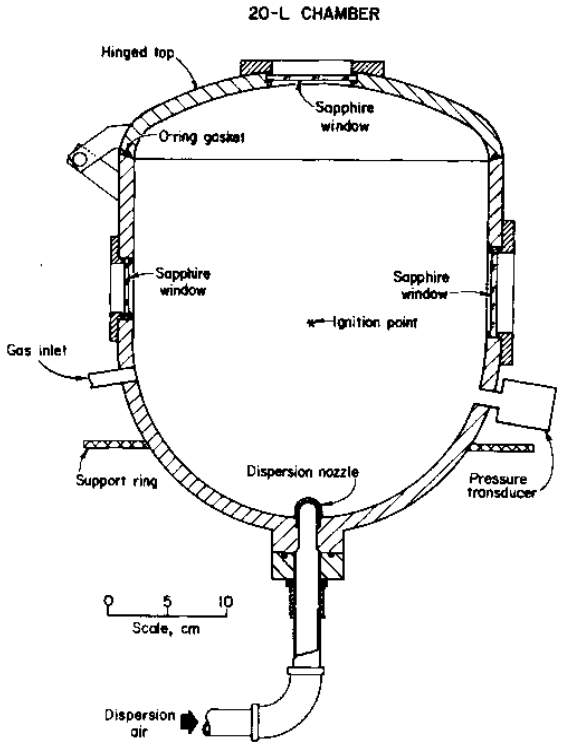

Fig. 2. 20 L flammability test chamber

gases. In other tests, a fan was used to mix the gases. The spark electrodes were located slightly below center.

The calibrations of the pressure transducers for both the 20 L and 120 L chambers were checked daily using the internal shunt calibration resistors provided by the manufacturers. At the start of a test, the chamber was evacuated, and then the fuel gas and air were added at the partial pressures required to give the desired mixture composition. A non-sparking internal fan was used for mixing the gases in the 120 L chamber and for some of the tests in the 20 L chambers. When the fan was used, the gases were mixed for at least 3 to 4 minutes before each test, and the fan was turned off 1 minute prior to ignition to provide a well mixed, quiescent system. The absolute pressure at ignition was about 1 bar or 1 atm. Samples of the gas mixtures could be collected in evacuated test tubes through a sampling needle on the side of the chamber. These samples would then be analyzed by gas chromatography (GC). During the initial evaluation of the mixing efficiency in the 120 L chamber, samples of H_2-air mixtures were collected at t=0 min (after all of the gases had been added to the chamber) and after 2 and 5 min of mixing by the fan. There was essentially no difference in the measured concentrations of H_2 for the gas mixtures over this time period, showing that there was good mixing of the gases even before the fan was turned on. For some of the H_2 tests in the 20 L chamber, the fuel gas was added first and then the air was added rapidly through the solenoid valve as a way of mixing the gases. The data showed no difference from the fan mixed case. The reported fuel concentrations are in mole (volume) percent, based on the partial pressure of the fuel relative to the total pressure.

Both the 20 L and 120 L chambers had similar spark ignition systems. The electrodes were 3 mm diameter brass rods. In some cases, the brass rods were sharpened to a point. In other cases, steel phonographic needles were soldered to the ends of the rods. The electrodes were positioned slightly below center in the chambers, with a spark gap of 6 mm. For the 20 L tests, a 380 or 900 μf capacitor was charged to 300 V and then discharged through a transformer to generate a strong spark with a stored energy ($\frac{1}{2}CE^2$, where C is the capacitance and E is the voltage) of 17 or 40 J. The actual electrical energy in the spark gap may have been considerably less because of the low efficiency of the transformer circuit (Hertzberg, Conti, & Cashdollar, 1985). In the 20 L chamber, the measured pressure pulse due to the rapid heating (by the spark) of the air volume in the immediate vicinity of the electrode gap was ~0.3 mbar. The corresponding delivered thermal energy (2.5 $V\Delta P$, where V is the chamber volume and ΔP is the pressure rise) was about 1 J. For the 120 L tests, the standard ignition source was a strong electric spark from a 1300 μF capacitor at 300 V. This corresponded to a stored energy on the capacitor of $\frac{1}{2}CE^2$ =58 J. The thermal energy of this spark was about 2 J, based on the measured pressure rise in a known volume. For practical comparisons, Lüttgens and Glor (1989: 159) and Eckhoff (1991: 17) report typical electrostatic spark energies in industrial practice of 15 mJ for a person to several hundred millijoules for major plant items such as large containers.

Much stronger, electrically-activated, pyrotechnic ignitors with calorimetric energies of 1000 to 5000 J were used for some of the tests in the 120 L chamber. These ignitors produce a large flame of hot particles; they are manufactured by Fr. Sobbe[3] of Dortmund, Germany and distributed by Cesana Corp. of Verona, NY. The energy of the 5000 J ignitor is somewhat higher than that of two books of pocket matches, all ignited at once.

For a test with initially "turbulent" conditions in the 120 L chamber, the mixing fan was left on during the test. The fan was located near the bottom flange as shown in Fig. 1, and the gas flow was directed toward the ignition point. The fan had an 8 cm diameter blade that rotated at 3000 rpm. The flow characteristics of the fan were measured in open air outside the chamber. The air flow velocity along the axis of rotation was ~1.4 m/s at 15 cm, ~1.1 m/s at 30 cm, and ~0.7 to ~1.1 m/s at 45 cm from the fan blade. The turbulence level generated by the fan was not directly measured; the fan was used only to determine whether moderate turbulence had a significant effect on the flammability data of the various gases near the lower flammable limit.

The data from the pressure transducers, the flame sensor, and the thermocouple were recorded using a high speed analog-to-digital (A/D) board in a personal computer (PC). This system can sample the data from various instrument channels, usually at speeds less than 20 kHz per channel. A PRL designed computer software program converted the raw data to engineering units, plotted the data versus time, and allowed various data smoothing options. Maximum pressure and maximum rate of pressure rise values were obtained from the pressure versus time traces. Data from the two pressure transducers were compared and averaged if they agreed to within 5%. If they did not agree to within 5%, the two pressure transducers were checked to determine the reason for the difference. The reproducibility of the flammability data was checked by repeat tests over a period of months or years.

Some earlier PRL data by other researchers (Furno, Cook, Kuchta, & Burgess, 1970; Nagy, Seiler, Conn, & Verakis, 1971; Sapko, Furno, & Kuchta, 1976; Burgess, Furno, Kuchta, & Mura, 1982) in a much larger 25.5 m^3 chamber are included for comparison purposes. This spherical chamber had an internal diameter of 3.65 m

[3] Mention of any company name or product does not constitute endorsement by NIOSH.

and a pressure rating of 21 bar. Also included for comparison are some previously published hydrogen data (Hertzberg & Cashdollar, 1983) and some previously unpublished methane data from an 8 L cylindrical chamber (Hertzberg, Cashdollar, Lazzara, & Smith, 1982), which had a diameter of about 19 cm and a height of about 30 cm.

3. Thermodynamic calculations

Adiabatic equilibrium calculations of product gas temperatures, pressures, and compositions were made for the various fuel gas and air mixtures. The calculations give the maximum expected explosion temperatures and pressures for the gas mixtures in the absence of a detonation. A comparison of the experimentally measured pressures with the calculated adiabatic pressures would indicate the extent of reaction of the fuel-air mixture and the degree of adiabaticity of the explosion.

The calculations were generated on Digital Electronic Corp. VAX computers using the CEC-80 Fortran code for the computation of complex equilibrium calculations that was developed at the NASA-Lewis Research Center (Gordon & McBride, 1976). This program computes the equilibrium product composition from the listed reactants and their standard energies of formation by examining all possible product species (consisting of combinations of the reactant atoms) whose temperature dependent thermodynamic properties are listed in an auxiliary table. The thermodynamic properties accessed by the program are taken predominantly from the JANAF thermodynamic data compilation (Chase, Davies, Downey, Frurip, McDonald, & Syverud, 1985). The product composition is obtained by minimizing the free energy of the system. The associated adiabatic flame temperature is also determined for each system. Constant volume calculations were used to compare the experimentally measured pressures to the adiabatic equilibrium pressures. Constant pressure calculations were also performed at one atmosphere to determine the corresponding adiabatic temperatures. Such temperature calculations have been found useful in deriving limiting flame temperatures and compositions.

4. Experimental data

4.1. Pressure traces for methane and hydrogen

Fig. 3 shows the pressure rise versus time traces for various gaseous mixtures of CH_4 and air, tested in the 120 L chamber. The mixtures were initially quiescent and a spark ignition source was used. Fig. 3A shows data for a mixture of 5% CH_4 and 95% air. The pressure-time trace shows only a small pressure rise (~0.06 bar)

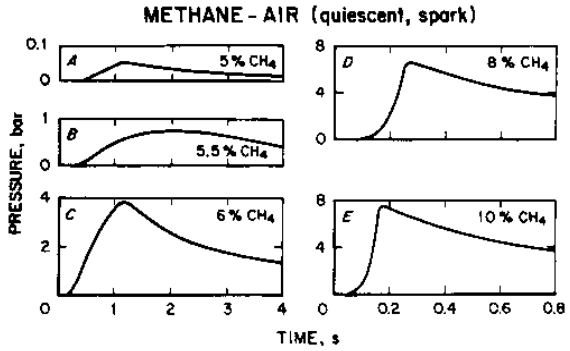

Fig. 3. Pressure-time traces for mixtures of (A) 5% CH_4 in air, (B) 5.5% CH_4 in air, (C) 6% CH_4 in air, (D) 8% CH_4 in air, and (E) 10% CH_4 in air.

and is typical of a mixture on the edge of flammability. There may be some burning near the spark but only limited upward propagation beyond the ignition source. The data in Fig. 3B are for 5.5% CH_4 and 94.5% air. For this test, there is a ~0.7-bar pressure rise associated with upward and horizontal flame propagation. Upward propagation is easier than other propagation directions because combustion products are hotter and less dense than the reactants from which they are generated. The upward acceleration of the burned gas flame kernel aids upward flame propagation (Hertzberg, Cashdollar, Litton, & Burgess, 1978; Hertzberg, 1976). Hence, upward propagation is always easier in the sense that leaner mixtures that can propagate upward may not be able to propagate downward. That is the case for the 5.5% CH_4 mixture in Fig. 3B. The data in Fig. 3C are for 6% CH_4 and 94% air. For this test, there is a pressure rise of almost 4 bar, and there is significant flame propagation in the horizontal and downward directions in addition to upward. At 6% CH_4, the calculated pressure rise for adiabatic combustion is about 5.9 bar. Therefore, the flame had to propagate through more than half of the chamber in this case.

The data in Fig. 3D are for 8% CH_4 and 92% air. For this test, the propagation is rather rapid and nearly spherical. The measured peak explosion overpressure (~6.5 bar) is close to the calculated, adiabatic equilibrium pressure (7.2 bar) for constant volume combustion, and most of the mixture is consumed. The data in Fig. 3E are for 10% CH_4 and 90% air. For this near-stoichiometric mixture, the flame speed is fast, and it takes less than 0.2 s for the flame to propagate from its point of ignition to the chamber wall (a distance of 30 cm). The measured peak explosion overpressure (~7.5 bar) is close to the calculated, adiabatic equilibrium pressure (7.9 bar) for constant volume combustion, showing that the entire mixture is almost completely consumed.

Fig. 4 shows the pressure rise versus time traces for various quiescent mixtures of H_2-air, tested in the 120 L

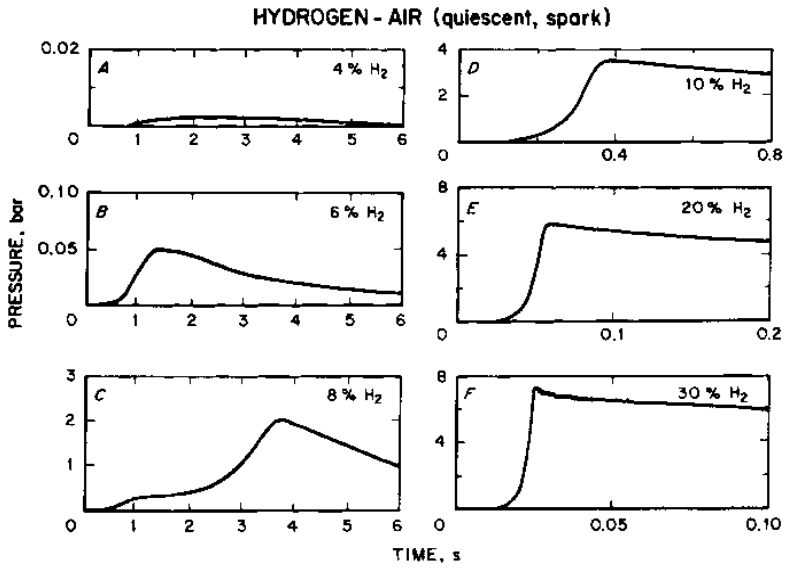

Fig. 4. Pressure-time traces for mixtures of (A) 4% H_2 in air, (B) 6% H_2 in air, (C) 8% H_2 in air, (D) 10% H_2 in air, (E) 20% H_2 in air, and (F) 30% H_2 in air.

chamber using a spark ignition source. Fig. 4A shows data for a mixture of 4% H_2 and 96% air. The pressure-time trace shows only a very small pressure rise (~0.002 bar). This would not be considered propagation for most pressure rise criteria. The data in Fig. 4B are for 6% H_2 and 94% air. There is a small but measurable pressure rise (~0.05 bar) associated with propagation in the upward direction only. Hydrogen is an unusual fuel with both high reactivity and high diffusivity. The actual concentration at the surface of the highly curved and discrete flame kernels is appreciably higher than the overall concentration (Coward & Jones, 1952; Hertzberg 1982, 1989). At low H_2 concentrations, these highly buoyant, ascending flame kernels can propagate for significant distances while barely affecting the overall gas temperature, pressure, and composition (Coward & Jones, 1952).

The data in Fig. 4C are for a mixture containing 8% H_2 and 92% air, and the propagation is a two stage process. The early stage of the pressure-time trace is associated with upward and horizontal flame propagation. A pause in the pressure rise occurs from 1 to 2 s at a pressure of ~0.3 bar as the upward propagating flame front reaches the top of the spherical chamber. The later, more rapid downward flame propagation results in the peak pressure of 2.0 bar at a time of 3 to 4 s. This shows that there is a transition to downward flame propagation at ~8% H_2.

The data in Fig. 4D are for a mixture containing 10% H_2 and 90% air. For this composition, the propagation dynamics are simpler and essentially isotropic. The propagation is rapid and nearly spherical, as seen by the continuous increase in pressure with time. Combustion is essentially complete before 0.4 s. The measured peak explosion overpressure (3.2 bar) is essentially the same as the calculated, adiabatic equilibrium pressure for constant volume combustion. The entire mixture is almost completely consumed as the spherical fireball reaches the wall almost simultaneously for all three directions of flame propagation (upward, downward, and horizontal). The pressure time trace in Fig. 4E is for a mixture containing 20% H_2 and 80% air. For this mixture, the flame speed is very fast, and it now takes slightly less than 0.06 s for the flame to propagate from its point of ignition to the chamber wall (a distance of 30 cm). The measured peak explosion overpressure (5.6 bar) is essentially the same as the calculated, adiabatic equilibrium pressure. The pressure time trace in Fig. 4F is for a mixture containing 30% H_2 and 70% air. Here the flame speed is even faster and the high frequency pressure fluctuations (acoustic ringing) may be the start of a transition to a detonation. Again, the measured explosion pressure is essentially the same as the calculated adiabatic pressure.

4.2. *Methane-air, quiescent, spark*

A graphical summary of the data for mixtures of methane (CH_4) and air tested in the 20 L and 120 L chambers using spark ignition is shown in Fig. 5. At the bottom of the figure, the pressure ratio, *PR*, is the maximum absolute explosion pressure for each test divided by the initial absolute pressure:

$$PR = P_{max}/P_{initial} \quad (1)$$

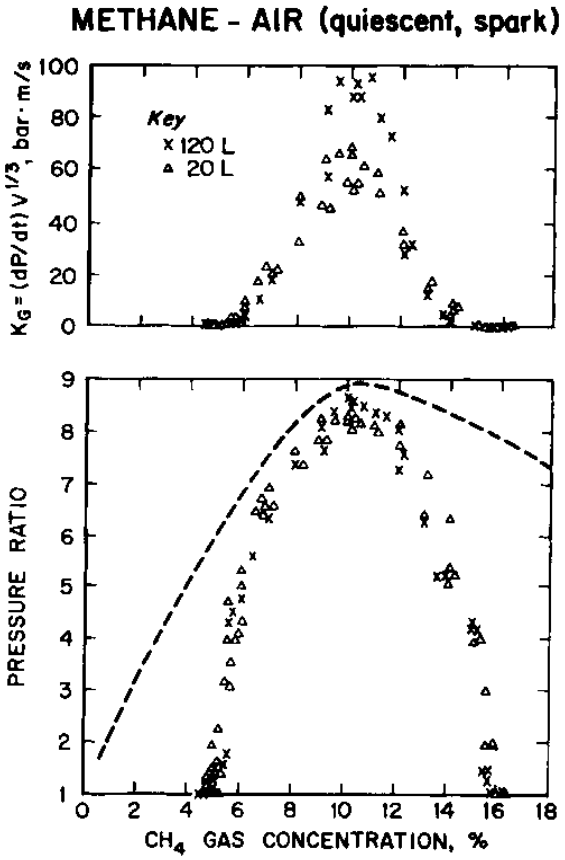

Fig. 5. Flammability data for quiescent mixtures of methane (CH_4) in air in 20 L and 120 L chambers, compared to dashed curve for calculated adiabatic values.

Since the initial pressure for a test is approximately one bar or one atmosphere, the pressure ratio is approximately the absolute explosion pressure in bars or atmospheres. Subtracting the number 1 from the pressure ratio value would give the explosion pressure rise in bars or atmospheres. Taking the ratio of explosion pressure to initial pressure is a way of normalizing the data and correcting for slight variations in the starting test pressure. At the top of the figure, K_G is the maximum rate of pressure rise, $(dP/dt)_{max}$, for each test, normalized by the cube root of the chamber volume, V:

$$K_G = (dP/dt)_{max} V^{1/3} \quad (2)$$

These CH_4 data in Fig. 5 are typical of those for hydrocarbon gases. There is a sharp discontinuity at the lower flammable limit near 5% and at the upper flammable limit near 16%. The explosion pressures and rates of pressure rise are highest at a concentration (~10%) that is slightly above the stoichiometric value of 9.5%. The pressure data for spark ignition in the two chambers are very similar, and the peak explosion pressures at ~10% CH_4 are close to the calculated, adiabatic equilibrium values (dashed curve). The 120 L peak pressures are slightly higher than those from the 20 L chamber, showing that the 120 L chamber explosions are more adiabatic. The normalized rates of pressure rise (K_G) in the two chambers are similar near the flammability limits, but the K_G-data from the larger chamber are higher near stoichiometric CH_4 concentrations. The most likely reason is that near-stoichiometric flame propagation in the larger, spherical chamber more nearly approximates ideal, adiabatic combustion.

The lean flammability limit region of Fig. 5 is shown in more detail in the expanded scale of Fig. 6. This graph compares the 120 L data to earlier data (Burgess et al., 1982) from a 25.5 m^3 chamber at PRL. A reasonable criterion used previously (ASTM, 1999) for upward flame propagation in air (using a spark ignition source in a closed vessel) is a pressure rise of at least 0.07 bar (1 psi) or at least 7% higher than the initial pressure of 1 bar. This corresponds to $PR \geq 1.07$. Based on this propagation criterion, the lean flammable limit for upward flame propagation of methane in air in the 120 L chamber is $LFL = 5.0 \pm 0.1\%$, using spark ignition. In the much larger 25.5 m^3 chamber, the LFL is $5.1 \pm 0.1\%$ using the same pressure rise criterion. However, Burgess et al. (1982) reported visual observations of upward flame travel at methane concentrations as low as 4.9% in the 25.5 m^3 chamber. The LFL values with either a

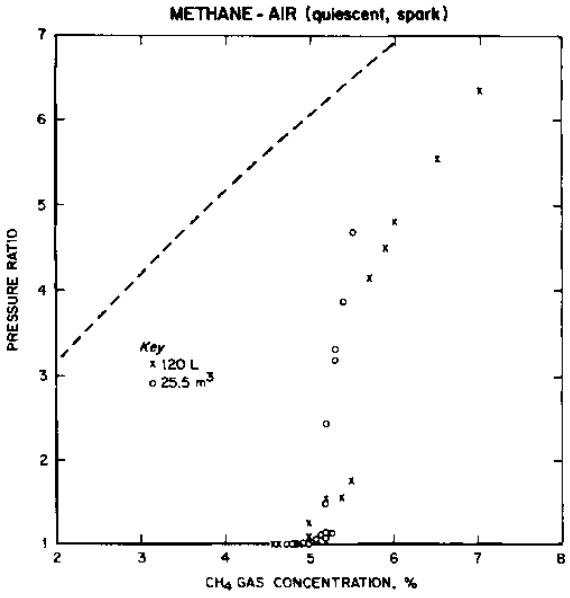

Fig. 6. Lean limit flammability data for quiescent mixtures of methane in air in 120 L chamber, compared to earlier data from 25.5 m^3 chamber (Burgess et al., 1982) and to dashed curve for calculated adiabatic values.

pressure rise or visual criterion are consistent with the 5.0% *LFL* reported for upward propagation of methane-air flames in flammability tubes (Kuchta, 1985).

4.3. Methane-air, turbulent, spark

The data shown in Fig. 7 are for "turbulent" combustion of CH_4-air mixtures in the 120 L chamber. The initial turbulence level was induced by allowing the mixing fan to run continuously during the 120 L test. The purpose of these tests was to determine the effects of a moderate initial gas flow or turbulence on the flammability data at low CH_4 concentrations. These "turbulent" data (open circles) are compared with the data (solid curve) for the quiescent CH_4-air mixtures from Fig. 6. The calculated adiabatic explosion pressure is again shown as the dashed curve. The measured pressure ratio data indicate that there is no significant difference between the "turbulent" and quiescent cases for CH_4-air near the lean limit.

4.4. Methane-air, quiescent, pyrotechnic ignitors

Fig. 8 shows CH_4-air data for 1000 and 5000 J ignitors in the 120 L chamber. The experimental pressure data are again compared to the quiescent spark data (solid curve) and to the calculated, adiabatic equilibrium pressures (dashed curve). The pressure rise from the ignitor by itself was subtracted from the measured pressure for the data in the figure.

$$PR=(P_{max}-\Delta P_{ignitor})/P_{initial} \quad (3)$$

For the 1000 J ignitors, this pressure was 0.025 bar and for the 5000 J ignitors, it was 0.09 bar. The apparent lean limits using the Sobbe ignitors are somewhat lower than that measured with the electric spark source. However, the stronger Sobbe pyrotechnic ignitors have a much larger ignition volume than the spark, and all of the CH_4 in this volume would be combusted even without any propagation beyond the ignition volume. Therefore, it is reasonable to use a more stringent pressure rise criterion for flame propagation with the Sobbe ignitors. For this study, a criterion of $PR \geq 1.5$ for upward propagation was chosen. (In previous studies using the 20 L chamber (Hertzberg et al., 1988), a criterion of $PR \geq 2$ was used for the Sobbe ignitors since the ignitor volume represents a larger fraction of the 20 L chamber volume than for the 120 L chamber.) Using this $PR \geq 1.5$ criterion, the methane-air limits in the 120 L chamber

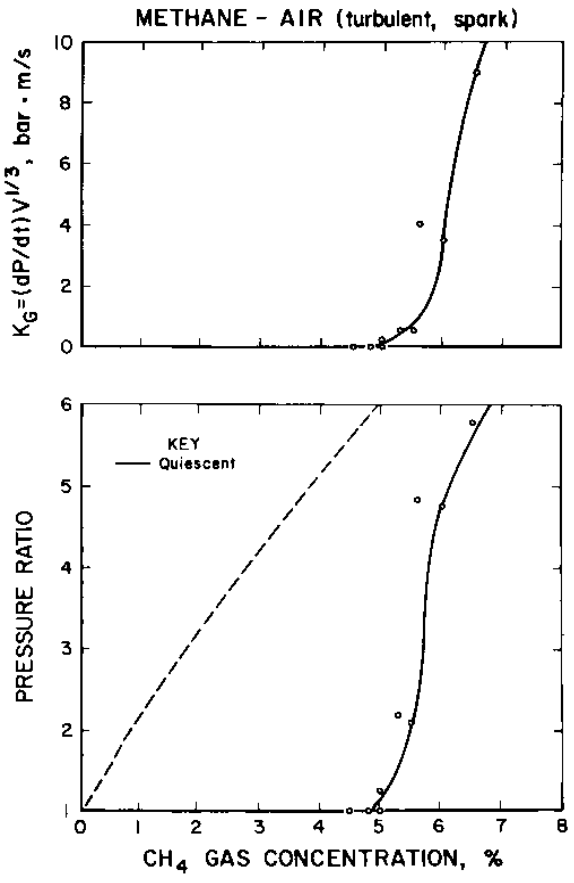

Fig. 7. Lean limit flammability data (open circles) for "turbulent" mixtures of CH_4 in air in 120 L chamber, compared to solid curve for quiescent experimental data and to dashed curve for calculated adiabatic values.

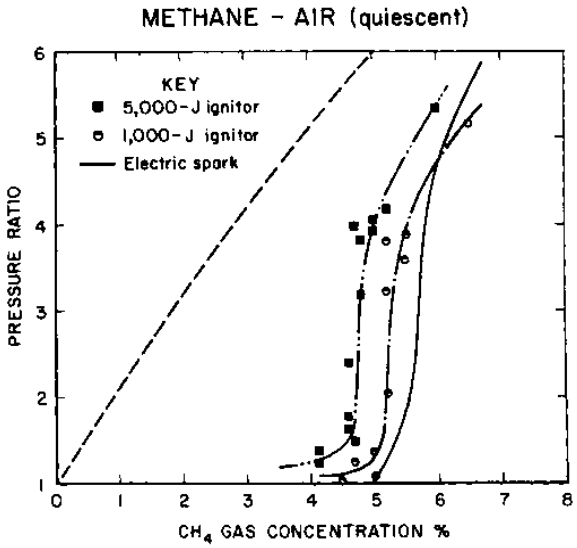

Fig. 8. Flammability data for quiescent mixtures of CH_4 in air in 120 L chamber, using 1000- or 5000 J pyrotechnic ignitors, compared to solid curve for spark data and to dashed curve for calculated adiabatic values.

are: *LFL* =4.6% for the 5000 J ignitor and *LFL* =5.1% for the 1000 J ignitor. The lower *LFL* with the 5000 J ignitor indicates that this high energy pyrotechnic is "overdriving" the mixture somewhat in the 120 L chamber. The final conclusion for the methane-air data is that there is no major difference in the measured lean limit results with the different strength ignitors or for upward versus downward propagation.

4.5. Propane-air, quiescent, spark

The data for initially quiescent mixtures of propane (C_3H_8) in air shown in Fig. 9 are similar in form to the methane-air data in Fig. 5. There is a sharp discontinuity at the lower flammable limit near 2%. There is a fairly distinct drop in pressure near 8% C_3H_8, but there is also a tail of measurable pressures out to higher C_3H_8 concentrations. Based on a pressure rise criterion of 7% or $PR \geq 1.07$, the *LFL* of propane is 2.05±0.05% and the *UFL* is ~9.8±0.2%. These limits correspond to upward flame propagation that consumes only a small fraction of the flammable gas mixture. The *LFL* for downward propagation would be slightly above 2% since the discontinuity is very sharp at the *LFL*. However, the *UFL* for downward propagation would be 7.5% to 8% C_3H_8, significantly lower than the *UFL* for upward propagation. This is probably due to the greater diffusivity (Hertzberg, 1989) of oxygen (0.43 cm^2/s) relative to that of propane (0.25 cm^2/s). The oxygen can selectively diffuse into the flame front, enriching it in oxygen. This effect could allow rich mixtures that would not normally be flammable to propagate upward in a narrow cone angle. A similar effect was observed for the *UFL* of *n*-butane in Furno et al., 1970 and Burgess et al., 1982.

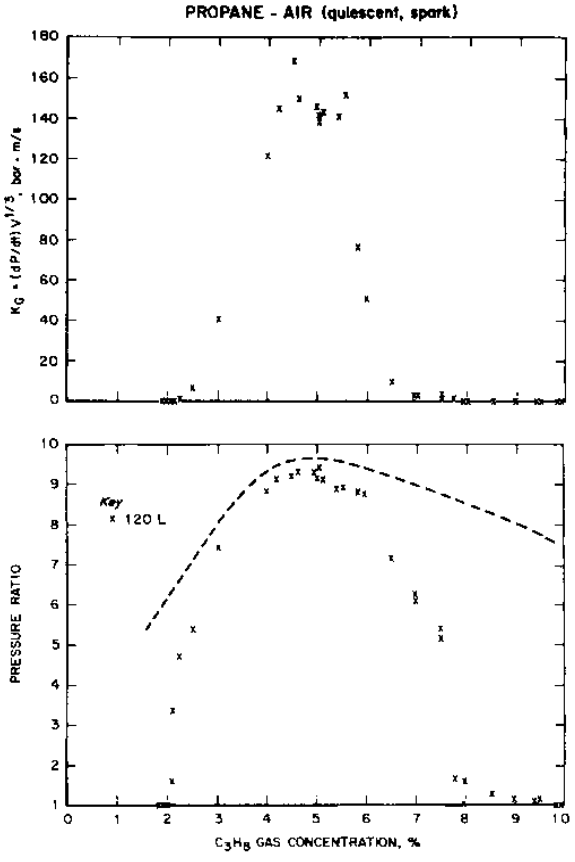

Fig. 9. Flammability data for quiescent mixtures of propane (C_3H_8) in air in 120 L chamber, compared to dashed curve for calculated adiabatic values.

In Fig. 9, the propane explosion pressures and rates of pressure rise are highest at a concentration (~4.5% to 5%) that is slightly above the stoichiometric value of 4.0%. The maximum explosion pressures are close to the calculated adiabatic values. The maximum explosion pressures for the propane are somewhat higher than those for methane, in accord with its higher reactivity. The maximum K_G values for the propane-air mixtures are considerably higher than those for methane-air.

4.6. Hydrogen-air, quiescent, spark

The data for initially quiescent hydrogen-air mixtures with spark ignition in the 120 L chamber are shown in Fig. 10. The measured peak explosion pressure ratios and the size normalized rates of pressure rise are plotted as a function of hydrogen concentration in air. The measured pressure ratios are compared with the calculated, adiabatic equilibrium explosion pressures for constant volume combustion (dashed curve). For hydrogen concentrations above 10% where the propagation is rapid and isotropic and the complications associated with buoyancy are minimal, there is very good agreement between the measured pressure ratios and those calculated for adiabatic equilibrium. The maximum explosion pressures and rates of pressure rise are found at a H_2-concentration that is somewhat above the stoichiometric value of 29.5%.

The lower concentration H_2-data are shown in an expanded scale in Fig. 11. The pressures are very low at concentrations less than 8% H_2. The complexities associated with low H_2 concentrations have already been discussed in relation to the pressure time traces shown in Fig. 4. The data for the H_2-air mixtures shown in Fig. 11 display essentially the same combination of two stage flame propagation at ~8% H_2. There is a rapid increase in the measured pressure ratio at ~8% H_2, and that near-discontinuity corresponds to the lean limit for downward flame propagation. In the earlier PRL hydrogen tests in the 25.5 m^3 sphere (Furno et al., 1970), the limit for downward flame propagation was slightly higher, ~8.5% H_2. As indicated earlier, in the presence of buoyancy, complete consumption of the unburned mixture is poss-

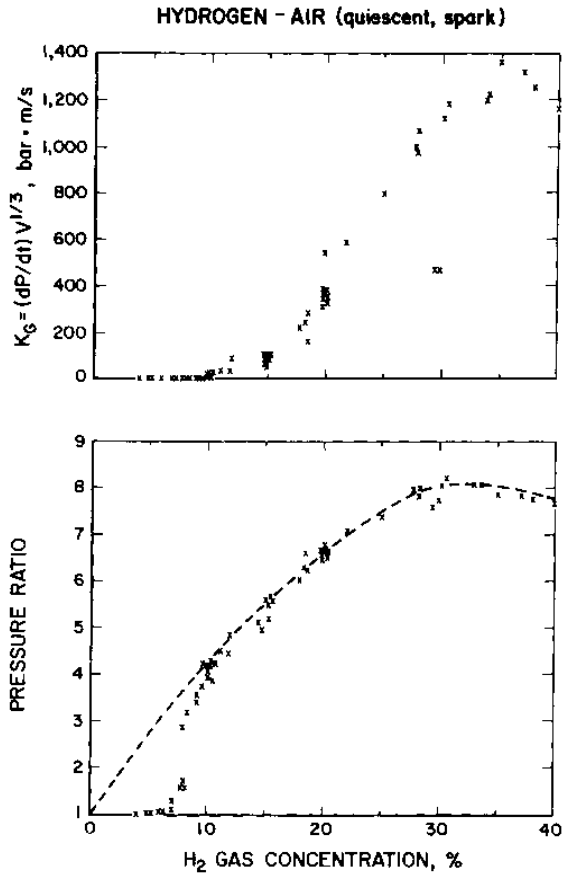

Fig. 10. Flammability data for quiescent mixtures of hydrogen (H_2) in air in 120 L chamber, compared to dashed curve for calculated adiabatic values.

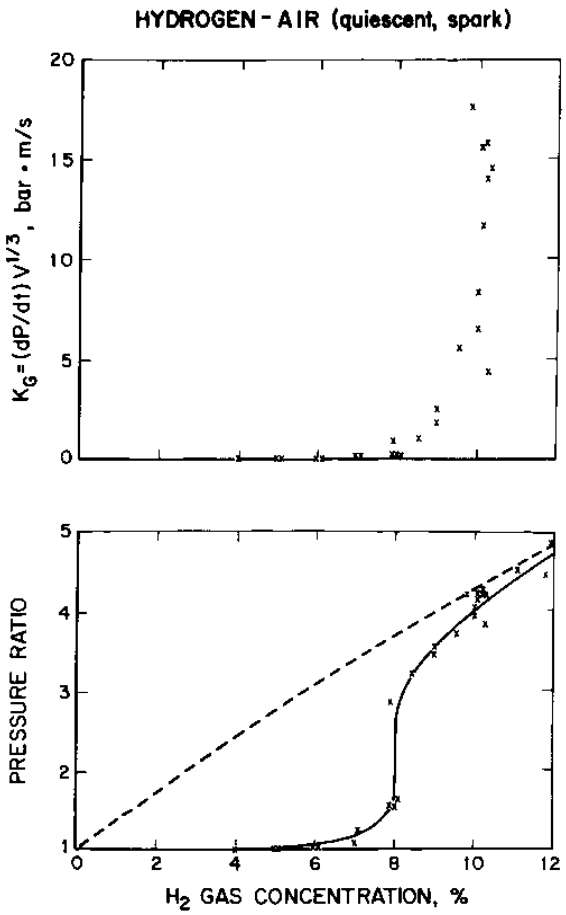

Fig. 11. Expanded scale flammability data for quiescent mixtures of hydrogen in air in 120 L chamber, compared to dashed curve for calculated adiabatic values.

ible in the sphere only if the downward propagation occurs. Once that downward lean limit is exceeded (H_2 >8%), complete combustion is possible, and the measured explosion pressures approach the calculated adiabatic values at ~10% H_2.

Hydrogen flammability data from the 20 L and 120 L chambers over the 3% to 9% H_2 region are shown on a greatly expanded scale in Fig. 12. For concentrations less than the downward limit of ~8% H_2, only upward propagation is possible in the quiescent mixture. This upward propagation occurs in a narrow cone angle above the spark. For concentrations <8% H_2, the volume of the unburned mixture consumed in that cone angle is so much smaller than the total spherical test volume that measured pressures are only a small fraction of the calculated adiabatic values for complete combustion (Fig. 11). As the concentration increases from 4% to 8%, the cone angle and volume of burned gases increases gradually, resulting in a gradual increase in pressure. The ability of hydrogen to propagate flame in an upward direction at such low concentrations is remarkable. A H_2 concentration of 5% corresponds to a fuel equivalence ratio of 0.17 compared to 0.53 at the *LFL* of 5% for CH_4. An explanation for this phenomenon of H_2 flame propagation below 8% is that fresh hydrogen selectively diffuses into the flame front more rapidly than oxygen does, thus enriching the flame in hydrogen (Coward & Jones, 1952; Hertzberg 1982, 1989; Goldmann, 1929). The diffusivity of hydrogen is 1.86 cm^2/s, much larger than the 0.43 cm^2/s value for oxygen (Hertzberg, 1989). Based on the previous criterion of a 7% pressure rise or $PR \geq 1.07$, the *LFL* = 6.0±0.5% for H_2-air in the 20 L chamber and *LFL* = 6.5±0.5% for H_2-air in the 120 L chamber, using a spark ignition source. Based on a weaker criterion of a 0.03 bar (0.5 psi) or 3% pressure rise used in some previous studies (Zlochower, Cashdollar, & Green, 1997), the *LFL* = 5.0±0.5% for H_2-air in both the 20 L and 120 L chambers. These values are still higher than the *LFL* of 4% H_2 reported from

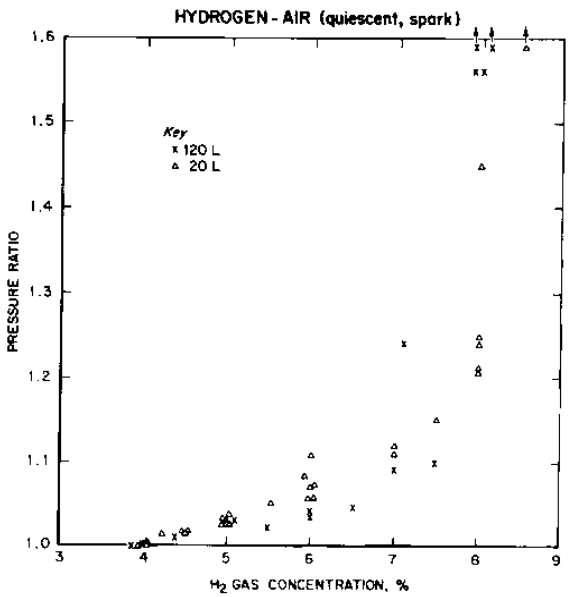

Fig. 12. Lean limit flammability data for quiescent mixtures of hydrogen in air in 20 L and 120 L chambers.

flammability tubes (Kuchta, 1985; Kumar, 1985), using a visual criterion for upward flame propagation. In Fig. 12, 4% H_2 corresponds to a point where the pressure versus H_2 concentration data curve reaches the x-axis at PR =1.0 or at a pressure rise of 0.0 bar.

4.7. Hydrogen-air, turbulent, spark

The data shown in Fig. 13 are for "turbulent" combustion of H_2-air mixtures. The initial turbulence level was induced by allowing the mixing fan to run continuously during the 120 L test. The purpose of these tests was to show the effects of moderate initial gas flow or turbulence on the flammability data at low H_2-concentrations. These "turbulent" data (open circles) are compared with the solid curve data for the quiescent H_2-air mixtures from Fig. 11. The calculated adiabatic explosion pressure is again shown as a dashed curve. The measured pressure ratio data points indicate that there is no significant difference between the "turbulent" and quiescent cases for H_2 concentrations above 10%, where the measured values under both initial conditions are close to the calculated adiabatic equilibrium explosion pressures. At the lower H_2-concentrations, however, there is no longer the sharp discontinuity associated with the downward limit near 8% H_2 that was observed for the quiescent (or laminar) case. Instead, for the "turbulent" case, there is an almost linear increase in the measured pressure between 4% and 10% H_2. At 6% H_2, the measured pressure rise for the "turbulent" case is over one-half the calculated, adiabatic value. For the quiescent case (solid

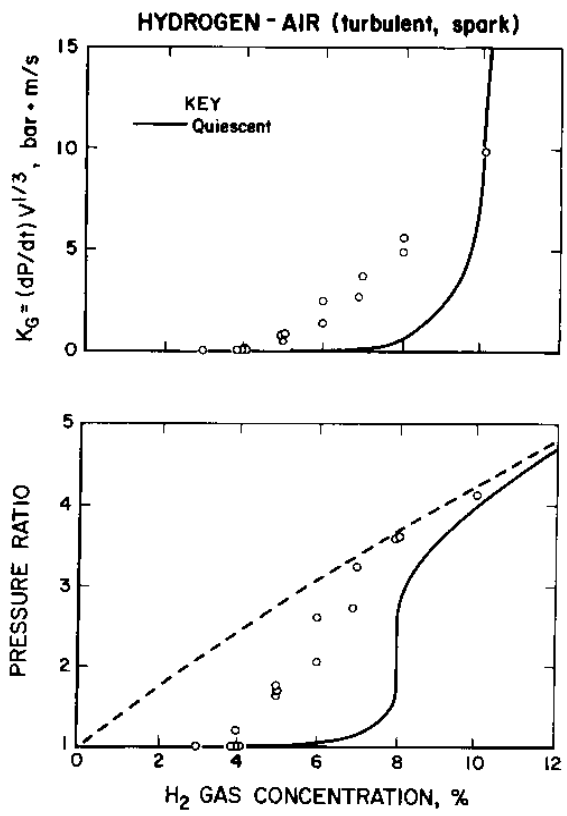

Fig. 13. Flammability data (open circles) near the LFL for "turbulent" mixtures of hydrogen in air in 120 L chamber, compared to solid curve for quiescent experimental data and to dashed curve for calculated adiabatic values.

curve in Fig. 13), the observed pressure rise at 6% H_2 is only a trivial fraction of the calculated, adiabatic value. The effect of turbulence is to increase the flame speed, which greatly reduces the limitations of buoyancy. This causes the propagation to be more isotropic, and the consumed flammable volume to be larger. Accordingly, the pressure rise for turbulent propagation in the transition zone is larger, as is observed in Fig. 13. An equivalent physical argument is to note that turbulence generates eddies of burned gas which are shed ahead of the flame-front in all directions. Eddies that are shed downward or in the horizontal direction or even upward can go well beyond the restricting cone angle, and they serve as multiple ignition sources that are absent for the quiescent, laminar case under buoyancy control. Based on the previous 7% pressure rise criterion, the turbulent $LFL \simeq 4\%$, comparable to the LFL for quiescent H_2-air in flammability tubes using a visual criterion (Kuchta, 1985). These data on the effects of turbulence on H_2 flammability are consistent with some earlier PRI. data (Hertzberg & Cashdollar, 1983) from an 8 L

chamber and those of other researchers (Cummings, Benedick, & Prassinos, 1983; Kumar, Tamm, Harrison, Skeet, & Swiddle, 1983).

4.8. Hydrogen-air, quiescent, 5000 J ignitor

The data in Fig. 14 are for H_2-air mixtures that were tested with a strong 5000 J pyrotechnic source in the 120 L chamber. To calculate the pressure ratios for the 5000 J ignitor tests in the 120 L chamber, the pressure rise of the ignitor by itself was subtracted from the maximum explosion pressure (Eq. (3)). However, as discussed for the CH_4 data, this did not correct entirely for the effects of the large ignitor flame. During a test, any H_2 gas that was within the ignitor flame would burn, regardless of whether flame would propagate beyond the ignitor. Therefore, even at 3 to 4% H_2, there was a measurable pressure ratio of 1.1 to 1.2 in Fig. 14. These low pressure ratios are not considered to be evidence of flame propagation when the 5000 J ignitors are used. Based on the previous criterion of $PR \geq 1.5$ for upward flame propagation with the Sobbe ignitors, $LFL \simeq 5.0 \pm 0.5\%$ under these test conditions. The 5000 J ignitor data further reinforce the viewpoints on turbulence from the preceding paragraphs because this pyrotechnic source induces turbulence in the test mixture. It also produces a large flame directed across the chamber toward the opposite wall rather than being a point source like the spark. Both of these effects negate the geometric limitations of buoyancy-controlled propagation from a point source. As a result, the data for the 5000 J pyrotechnic ignitor show a similar pressure increase versus H_2 concentration as was observed for the turbulent case (Fig. 13). The measured pressure for H_2-air with the 5000 J ignitor at 6% H_2 is about one-half the calculated adiabatic value.

In previous flammability experiments with the 5000 J ignitor in a 20 L chamber (Hertzberg, Cashdollar, & Zlochower, 1988) and in the data in Fig. 8 for CH_4 in the 120 L chamber, there was evidence that this strong ignitor could "overdrive" the system. The measured pressure ratios for H_2 mixtures at 4% and below shown in Fig. 14 are quite low, however, and suggest no significant overdriving for the 5000 J ignitor with H_2-air in the 120 L chamber. There is less "overdriving" by the 5000 J ignitors for the H_2 than for CH_4 (Fig. 8) since there is much less combustion energy available at 4% H_2-air than at 5% CH_4-air, as shown by the relative adiabatic pressures (dashed lines).

4.9. Deuterium-air, quiescent, spark

Deuterium (D_2), the heavier isotope of hydrogen, was tested to evaluate the effects of diffusivity on hydrogen flammability. Chemically, hydrogen and deuterium are virtually identical, but the lighter isotope's diffusivity is 1.86 cm^2/s, compared to 1.32 cm^2/s for deuterium (Hertzberg, 1989). The 120 L data obtained for initially quiescent D_2-air mixtures with spark ignition are shown in Fig. 15. The measured pressure ratios are compared with the experimental data for H_2-air mixtures (chain-dashed curve) and with the calculated, adiabatic equilibrium explosion pressures for constant volume D_2 combustion (dashed curve). In this case, the downward flame propagation limit has shifted from about 8% H_2 to about 9.5% D_2. Koroll and Kumar (1991) reported somewhat higher downward flame limits in a flammability tube: 9.0% for H_2 and 10.2% for D_2. The data in Fig. 15 show that selective diffusion has less of an effect for the deuterium than for the hydrogen, as expected due to its lower diffusivity. Based on the 7% pressure rise cri-

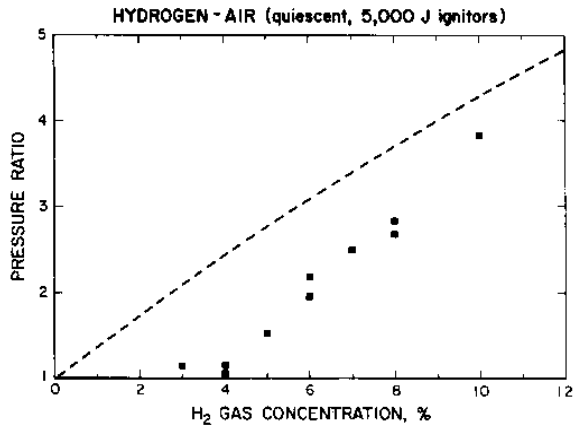

Fig. 14. Flammability data for quiescent mixtures of hydrogen in air in 120 L chamber, using 5000 J pyrotechnic ignitors.

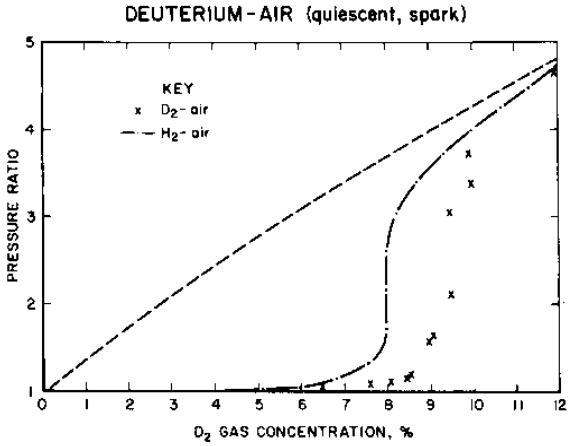

Fig. 15. Flammability data for quiescent mixtures of deuterium (D_2) in air in 120 L chamber, compared to dot-dashed curve for quiescent H_2-air and to dashed curve for calculated adiabatic values.

terion, the *LFL* ≃ 7.5±0.5% for upward flame propagation of D_2-air in the 120 L chamber, compared to the *LFL* ≃ 6.5±0.5% for H_2-air. Koroll and Kumar (1991) report upward flame limits in a flammability tube of 4.0% for H_2 and 5.6% for D_2, based on a visual criterion. Since the hydrogen and deuterium are essentially the same chemically, the differences in their flammability data have to be due to the differences in their diffusivities.

4.10. Deuterium-air, turbulent, spark

Deuterium-air was also tested as "turbulent" mixtures by allowing the fan to run during ignition (Fig. 16). The open circle data points for "turbulent" D_2-air show a similar effect to that of "turbulent" H_2-air (chain-dashed curve), but shifted to higher concentrations. Based on the 7% pressure rise criterion, the turbulent *LFL* ≃ 5.5% for D_2-air (compared to the *LFL* ≃ 4% for turbulent H_2-air). This *LFL* value for turbulent D_2-air is comparable to the *LFL* reported for D_2-air in flammability tubes, using a visual criterion (Koroll & Kumar, 1991).

5. Discussion and conclusions

A summary of the flammability limit data for methane, propane, hydrogen, and deuterium gases in air is listed in Table 1. All of the data were for initially quiescent mixtures, using spark ignition. The *LFL* values using a visual criterion for flame propagation were from earlier data in flammability tubes (Kuchta, 1985; Kumar, 1985; Koroll & Kumar, 1991) and in the 25.5 m^3 spherical chamber (Burgess et al., 1982). The *LFL* values using a pressure rise criterion of either 3% (0.5 psi) or 7% (1 psi) were from the present data in the 20 L and 120 L chambers and from earlier 8 L data (Hertzberg & Cashdollar, 1983) and 25.5 m^3 data (Furno et al., 1970; Burgess et al., 1982). The *UFL* data were from earlier flammability tube data (Kuchta, 1985) using a visual criterion and from the 8 L, 20 L, and 120 L data using a pressure rise criterion.

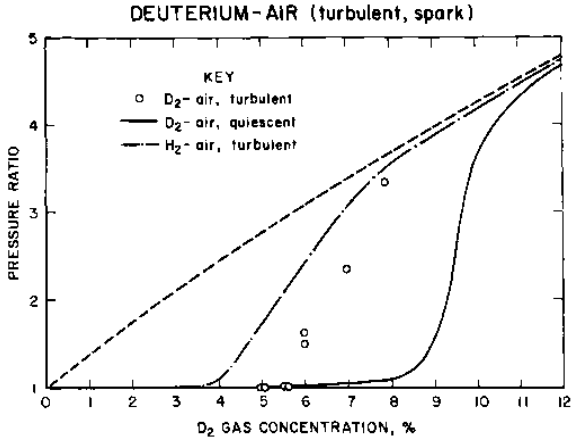

Fig. 16. Flammability data near the LFL for "turbulent" mixtures of deuterium in air in 120 L chamber, compared to solid curve for quiescent deuterium, to dot-dashed curve for "turbulent" hydrogen, and to dashed curve for calculated adiabatic values.

The methane *LFL* values show very close agreement, regardless of whether a visual criterion or a 3% or 7% pressure rise criterion is used. In all cases, the *LFL* for methane in air was close to 5.0% CH_4. The *UFL* for methane was somewhat higher in the 20 L and 120 L closed chambers than in the flammability tube. The propane *LFL* value from the 120 L chamber using either the 3% or 7% pressure rise criterion was comparable to the *LFL* from the flammability tube. The *UFL* for propane was slightly higher in the 120 L closed chamber than in the flammability tube.

The hydrogen data are listed in the fourth column of Table 1. The *UFL* for hydrogen in the 8 L chamber is somewhat higher than the value from flammability tube. The hydrogen *LFL* values show a large dependence on the propagation criterion chosen. The limit for visual observation of flame is about 4% H_2, but the measured pressure rise at this concentration is close to zero. Significantly higher H_2 concentrations are needed to reach a pressure rise of 7% (0.07 bar or 1 psi). The *LFL* for deuterium using the 7% pressure rise criterion was also higher than that measured in the flammability tube using a visual criterion. The data in the table also show that the hydrogen *LFL* based on this pressure criterion is higher in larger chambers. The *LFL* values were ~5%, 6.0%, 6.5%, and 7.5% for H_2-air in 8 L, 20 L, 120 L, and 25.5 m^3 chambers, respectively. An explanation of this systematic variation is that a fireball propagating only in the upward direction will constitute an increasingly smaller fraction of the chamber volume for larger chambers. Therefore, the corresponding pressure rise at a given H_2 concentration will be less in larger chambers. It follows that the flame propagation criteria chosen and consequently the resulting flammability limits are somewhat arbitrary. For practical applications of the flammability limit data, one should compare the measured pressures under various test conditions with the rated pressures of the vessels to be protected. The safety engineer must also consider quiescent conditions versus turbulent conditions (caused by obstacles), possible ignition sources, etc. The data in Figs. 13 and 14 show that the pressures are significantly higher over the 4% to 8% H_2 range under turbulent conditions or with a stronger ignition source. In using the *LFL* values, a safety factor must be included. NFPA 69 recommends (NFPA, 1997) that the fuel concentration be kept ≤25% of the *LFL*. The rationale for the safety factor is that fuel concentrations may vary throughout a vessel or area, and

Table 1
Flammable limits of gases (in volume %) for upward flame propagation in quiescent mixtures, with spark ignition

	Methane, CH_4	Propane, C_3H_8	Hydrogen, H_2	Deuterium, D_2
Lower Flammable Limit (LFL), using a visual criterion				
Flammability tube (Kuchta, 1985; Kumar, 1985; Koroll & Kumar, 1991)	5.0	2.1	4.0	5.6
25.5 m^3 sphere (Burgess et al., 1982)	4.9	–	–	–
Lower Flammable Limit (LFL), using pressure rise criterion of 3%				
20 L chamber	4.9±0.1	–	5.0±0.5	–
120 L sphere	5.0±0.1	2.05±0.05	5.0±0.5	–
Lower Flammable Limit (LFL), using pressure rise criterion of 7%				
8 L chamber (Hertzberg & Cashdollar, 1983)	5.0±0.1	–	~5±0.5	–
20 L chamber	5.0±0.1	–	6.0±0.5	–
120 L sphere	5.0±0.1	2.05±0.05	6.5±0.5	7.5±0.5
25.5 m^3 sphere (Furno et al., 1970 and Burgess et al., 1982)	5.1±0.1	–	7.5±0.5	–
Upper Flammable Limit (UFL), using a visual criterion				
Flammability tube (Kuchta, 1985)	15.0	9.5	75	–
Upper Flammable Limit (UFL), using pressure rise criterion of 7%				
8 L chamber (Hertzberg & Cashdollar, 1983)	–	–	76.8±0.2	–
20 L chamber	15.9±0.1	–	–	–
120 L sphere	15.7±0.2	9.8±0.2	–	–

Table 2
Maximum pressures and rates of pressure rise for gases

	Methane, CH_4	Propane, C_3H_8	Hydrogen, H_2
Maximum Pressures (P_{max}) in bar, g			
Calculated, adiabatic	7.9	8.6	7.1
20 L chamber	7.3±0.1	–	–
120 L sphere	7.5±0.1	8.2±0.2	7.1±0.1
25 m^3 sphere (Nagy et al., 1971; Sapko et al., 1976)	6.6±0.1[a]	7.8±0.5[a]	–
Maximum Rates of Pressure Rise (K_G) in bar·m/s			
20 L chamber	66±2	–	–
120 L sphere	92±3	150±20	1260±70
25 m^3 sphere (Nagy et al., 1971; Sapko et al., 1976)	110±8[a]	~400±100[a]	–

[a] Data at stoichiometric only.

the concentration at the measuring instrument may not be the worst case.

A summary of the maximum explosion pressures (P_{max}) and normalized rates of pressure rise (K_G) is listed in Table 2. Note that there were only a limited number of tests in the 25.5 m^3 sphere compared to the number of tests in the 120 L chamber in Figs. 5, 9 and 10. The maximum measured explosion pressures for methane-air and propane-air in the 120 L chamber were about 95% of the calculated values for adiabatic combustion. The P_{max} value for CH_4-air in the 20 L chamber was slightly lower. The measured explosion pressures in the 25.5 m^3 chamber (Nagy et al., 1971 and Sapko et al., 1976) were reported at stoichiometric concentrations, and may be slightly lower than would be found at concentrations slightly above stoichiometric. With this correction, the P_{max} value for C_3H_8-air in the 25.5 m^3 chamber would be close to the value in the 120 L chamber, but P_{max} for CH_4-air in the 25.5 m^3 chamber would still be lower than the value in the 120 L chamber. For H_2-air, which burns much faster than CH_4 or C_3H_8, the P_{max} value in the 120 L chamber is the same as the calculated, adiabatic value. The K_G values for CH_4-air show an increase with vessel size, perhaps due to greater flame induced turbulence in the larger chambers.

Acknowledgements

The authors wish to acknowledge the financial support of the U.S. Department of Energy and its site contractors Westinghouse Hanford Company and Lockheed Martin Idaho Technologies Company for parts of this research, particularly for the sections on hydrogen.

References

ASTM. (1999). *Standard practice for determining limits of flammability of chemicals at elevated temperature and pressure*. E918-

83. Vol. 14.02 in Annual Book of ASTM Standards. West Conshohocken, PA: American Society for Testing and Materials.

Burgess, D. S., Furno, A. L., Kuchta, J. M., & Mura, K. E. (1982). *Flammability of Mixed Gases*. Bureau of Mines RI 8709, 20 pp.

Cashdollar, K. L., Hertzberg, M., Zlochower, I. A., Lucci, C. E., Green, G. M., & Thomas, R. A. (1992). *Laboratory flammability studies of mixtures of hydrogen, nitrous oxide, and air*. Pittsburgh Research Center Final Report to DOE and Westinghouse Hanford Company, Richland, WA, June 1992, (published as WHC-SD-WM-ES-219, Revision 0, Westinghouse Hanford Company, Richland, WA, September 1992, 71 pp.)

Chase, M. W., Jr., Davies, C. A., Downey, J. R., Jr., Frurip, D. J., McDonald, R. A., & Syverud, A. N. (1985). *JANAF thermochemical tables (3rd ed.)*. (Thermal Group, Dow Chemical U.S.A., Midland, MI), Journal of Physical and Chemical Reference Data, v. 14, supplement 1.

Coward, H. F., & Jones, G. W. (1952). Limits of flammability of gases and vapors. *Bureau of Mines Bulletin, 503*, 155 pp.

Cummings, J. C., Benedick, W. B., & Prassinos, P. G. (1983). *Hydrogen combustion results from the Sandia intermediate-scale (VGES) tank and the Sandia critical-tube-diameter test facility*. Paper in Thermal-Hydraulics of Nuclear Reactors, v. II (pp. 1212–1218). LaGrange Park, IL: American Nuclear Society.

Eckhoff, R. K. (1991). *Dust explosions in the process industries*. Oxford: Butterworth Heinemann.

Furno, A., Cook, E. B., Kuchta, J. M., & Burgess, D. S. (1970). *Some observations on near-limit flames*. Paper in the Thirteenth Symposium (International) on Combustion (pp. 593-599). Pittsburgh, PA: The Combustion Institute.

Goldmann, F. (1929). Über difffusionserscheinungen an der unteren explosionsgrenze von wasserstoffknallgas (diffusion phenomena at the lower explosion limit of hydrogen-oxygen mixtures). *Z. Phys. Chem., B5*, 307–315.

Gordon, S., & McBride, B. J. (1976). *Computer program for calculation of complex chemical equilibrium compositions, rocket performance, incident and reflected shocks, and Chapman-Jouguet detonations*. NASA SP-273, 241 pp.

Hertzberg, M. (1976). *The theory of flammability limits: natural convection*. Bureau of Mines RI 8127, 15 pp.

Hertzberg, M. (1982). *The theory of flammability limits: radiative losses and selective diffusional demixing*. Bureau of Mines RI 8607, 38 pp.

Hertzberg, M. (1989). Selective diffusional demixing: occurrence and size of cellular flames. *Prog. Energy Combust. Sci., 15*, 203–239.

Hertzberg, M., & Cashdollar, K. L. (1983). *Flammability behavior and pressure development of hydrogen mixtures in containment volumes*. Paper in Thermal-Hydraulics of Nuclear Reactors, v. I (pp. 29–37). LaGrange Park, IL: American Nuclear Society.

Hertzberg, M., Cashdollar, K., Litton, C., & Burgess, D. (1978). *The diffusion flame in free convection. Buoyancy — induced flows oscillations, radiative balance, and large-scale limiting rates*. Bureau of Mines RI 8263, 33 pp.

Hertzberg, M., Cashdollar, K. L., Lazzara, C. P., & Smith, A. C. (1982). *Inhibition and extinction of coal dust and methane explosions*. Bureau of Mines RI 8708, 29 pp.

Hertzberg, M., Cashdollar, K. L., & Zlochower, I. A. (1988). *Flammability limit measurements for dusts and gases*. Paper in Twenty-First Symposium (International) on Combustion (pp. 303–313). Pittsburgh, PA: The Combustion Institute.

Hertzberg, M., Conti, R. S., & Cashdollar, K. L. (1985). *Electrical ignition energies and thermal autoignition temperatures for evaluating explosion hazards of dusts*. Bureau of Mines RI 8988, 41 pp.

Koroll, G. W., & Kumar, R. K. (1991). Isotope effects on the combustion properties of deuterium and hydrogen. *Combust. Flame, 84*, 154–159.

Kuchta, J. M. (1985). *Investigation of fire and explosion accidents in the chemical, mining, and fuel-related industries — a manual*. Bureau of Mines Bulletin 680, 84 pp.

Kumar, R. K. (1985). Flammability limits of hydrogen-oxygen-diluent mixtures. *J. Fire Sci., 3*, 245–262.

Kumar, R. K., Tamm, H., Harrison, W. C., Skeet, G., & Swiddle, J. (1983). *Combustion of hydrogen at high concentrations including the effect of obstacles*. Paper in Thermal-Hydraulics of Nuclear Reactors, v. II (pp. 1203–1211). LaGrange Park, IL: American Nuclear Society.

Lüttgens, G., & Glor, M. (1989). *Understanding and controlling static electricity*. Ehningen bei Böblingen, Germany: Expert Verlag.

Nagy, J., Seiler, E. C., Conn, J. W., & Verakis, H. C. (1971). *Explosion development in closed vessels*. Bureau of Mines RI 7507, 50 pp.

NFPA. (1997). National Fire Protection Association. *Standard on Explosion Prevention Systems* NFPA 69. Quincy, MA: National Fire Protection Association.

Sapko, M. J., Furno, A. L., & Kuchta, J. M. (1976). *Flame and pressure development of large-scale CH_4-Air-N_2 explosions*. Bureau of Mines RI 8176, 32 pp.

Zabetakis, M. G. (1965). *Flammability characteristics of combustible gases and vapors*. Bureau of Mines Bulletin 627, 121 pp.

Zlochower, I. A., Cashdollar, K. L., & Green, G. M. (September 1997). *Measurement of the lower flammability limits of mixtures of volatile organic compounds plus hydrogen in air*. Pittsburgh Research Center Final Report to Lockheed Martin Idaho Technologies Company, Idaho Falls, ID, September 1997, (published as Appendix B of INEEL/EXT-97-01073, *Flammability assessment methodology program phase i: final report*, by Loehr, C. A., Djordjevic, S. M., Liekhus, K. J., Connolly, M. J., Idaho National Engineering and Environmental Laboratory, Lockheed Martin Idaho Technologies Company, Idaho Falls, ID, September 1997).